Hindawi Publishing Corporation
Journal of Nanomaterials
Volume 2013, Article ID 421371, 7 pages
http://dx.doi.org/10.1155/2013/421371

Research Article

Oxide p-n Heterojunction of Cu_2O/ZnO Nanowires and Their Photovoltaic Performance

Seung Ki Baek, Ki Ryong Lee, and Hyung Koun Cho

School of Advanced Materials Science and Engineering, Sungkyunkwan University, Cheon Cheon-dong, 2066, Seobu-ro, Jangan-gu, Suwon-si, Gyeonggi-do 440-746, Republic of Korea

Correspondence should be addressed to Hyung Koun Cho; chohk@skku.edu

Received 6 July 2013; Accepted 21 August 2013

Academic Editor: Renzhi Ma

Oxide p-n heterojunction devices consisting of p-Cu_2O/n-ZnO nanowires were fabricated on ITO/glass substrates and their photovoltaic performances were investigated. The vertically arrayed ZnO nanowires were grown by metal organic chemical vapor deposition, which was followed by the electrodeposition of the p-type Cu_2O layer. Prior to the fabrication of solar cells, the effect of bath pH on properties of the absorber layers was studied to determine the optimal condition of the Cu_2O electrodeposition process. With the constant pH 11 solution, the Cu_2O layer preferred the (111) orientation, which gave low electrical resistivity and high optical absorption. The Cu_2O (pH 11)/ZnO nanowire-based solar cell exhibited a higher conversion efficiency of 0.27% than the planar structure solar cell (0.13%), because of the effective charge collection in the long wavelength region and because of the enhanced junction area.

1. Introduction

Cuprous oxide (Cu_2O) is an attractive material for the absorber layers of photovoltaic devices, because it has a direct band gap energy of 2.1 eV and a high absorption coefficient, which enable the fabrication of thin film solar cells [1]. In addition, Cu_2O solar cells have several advantages such as nontoxicity and low cost, compared with other types of thin film solar cells including copper indium gallium selenide solar cells [2]. To date, Cu_2O absorber layers have been prepared by techniques such as Cu thermal oxidation [3], anodic oxidation [4], sol-gel method [5], electrodeposition [6], and gas-phase deposition including sputtering and molecular beam epitaxy [7, 8]. Among these techniques, electrodeposition is a particularly attractive process because of its simplicity, scalability, and economy.

The electrical and optical properties of a Cu_2O absorber layer are significantly affected by the preferred orientation of a thin film, which varies according to bath pH and potential (or current density) [9–11]. These parameters also determine the grain size, crystallinity, and crystalline shape of the absorber layer during electrodeposition. Although the theoretical conversion efficiency of a Cu_2O-based solar cell was estimated to be about 20% [12], the experimental efficiency of a Cu_2O solar cell with a thermally oxidized Cu_2O layer and pulse-deposited ZnO layer was reported as 3.83% [13]. On the other hand, electrodeposited Cu_2O/ZnO heterojunction solar cells of 1.28% maximum efficiency could be obtained by controlling the current density of Cu_2O deposition [11]. But electrodeposited Cu_2O solar cells with a planar structure have problems such as low carrier concentration, small grain size, and short charge collection length [14]. Alternatively, nanostructured solar cells with oxide nanowires are expected to have improved charge collection efficiency because of the lower interval and higher contact area between the p-type and n-type materials. Recently, some studies on Cu_2O/ZnO nanowire heterojunction solar cells have been reported. However, in the case of Cu_2O deposited by the sputtering method on the ZnO nanowires, the Cu_2O layer did not fill the spaces between the nanowires [15]. Particularly, in Cu_2O/ZnO nanowires solar cells, the low conductivity of the solution processed ZnO nanowires increased the deposition time of the Cu_2O [16], which led to the contamination of the electrodeposition process.

In this study, we investigated the optimal electrodeposition condition of Cu_2O absorber layers by controlling bath

pH. The electrical, structural, morphological, and optical properties of the Cu_2O layers for different bath pHs were studied in detail. Also, the ZnO nanowire arrays were grown by metal organic chemical vapor deposition (MOCVD) to enhance the charge collection and reduce the defect states at the Cu_2O/ZnO interface.

2. Experiments

Indium tin oxide (sheet resistance of 10 Ω/sq) coated on a glass substrate (10 mm × 20 mm) was cleaned in ultrasonic baths with acetone, ethanol, and DI water for 20 min, respectively. Cuprous oxide films were cathodically electrodeposited from 0.4 M copper sulfate (98% anhydrous) and 3 M lactic acid (85% aqueous solution). The bath pH was controlled from 9 to 12 by addition of 4 M NaOH. Pt foil and Ag/AgCl (sat. NaCl) were used as the counterelectrode and the reference electrode, respectively. Electrodeposition was carried out at a fixed potential of −0.4 V (Ag/AgCl sat. NaCl) at 60°C using a Princeton applied research Versatate 4. Then, the deposition samples were rinsed with DI water and annealed at 150°C for 60 min to remove the contaminants. The morphological and structural properties of Cu_2O/ITO were examined by field-emission scanning electron microscopy (FE-SEM, JSM-7600F) operated at 10 kV and by the X-ray diffraction method (XRD, Bruker AXS D8 Discover) with CuK_α radiation source, respectively. The electrical properties of Cu_2O/ITO were investigated by current-voltage (I-V) measurements (HP4145B). And the optical absorption property of Cu_2O was analyzed by using a UV-VIS-NIR spectrophotometer (Varian Cary 5000).

Cu_2O/ZnO heterojunction solar cells with the structure shown in Figure 4(d) were fabricated. 5 at % Al doped ZnO (AZO) was deposited on the ITO/glass substrate by atomic layer deposition (ALD) at 200°C to prevent Cu_2O/ITO Schottky junction. The AZO thickness was 250 nm. ZnO nanowires were grown by MOCVD, which has been used to fabricate nanowire arrays of uniform length and shape, at 400°C and 1 Torr for 60 min using diethylzinc (DEZn) and high purity oxygen gas as precursor sources [17]. Also, n-type ZnO film of 300 nm thickness was deposited by the ALD process at 100°C. After the ZnO deposition, the p-type Cu_2O absorber layers were cathodically deposited on the n-type ZnO layers at pH 11, −0.4 V (Ag/AgCl sat. NaCl) at 60°C. Dark and illumination I-V curves were measured by a solar simulator with AM 1.5 G. External quantum efficiency measurements were performed using a 150 W Xe arc lamp light source, and Si photodiode was used for the light power density calibration.

3. Results and Discussion

Cu^{2+} species of copper sulfate stabilize in an alkaline solution and diffuse to the surface of a working electrode by an externally applied potential. The cathodic reduction of copper sulfate to Cu_2O consists of two reactions, reduction of Cu^{2+} to Cu^+ followed by the precipitation of Cu^+ into Cu_2O due to the low solubility of Cu^{2+} in water [18]. The overall reaction takes place as follows:

$$2Cu^{2+} + H_2O + 2e^- \longrightarrow Cu_2O + 2H^+ \quad (1)$$

This reaction depends on bath pH as confirmed in the Pourbaix diagram, a potential-pH predominance area diagram [19]. Because the bath pH affects the reaction potential and temperature, the solution pH is one of the key parameters that should be considered during an electrodeposition process.

Figure 1 shows the surface morphologies of the Cu_2O films electrodeposited on ITO, observed at 30° tilted-view, for bath pHs of 9, 10, and 11. As the bath pH increased, the concentration of hydroxyl ions in the electrodeposition condition increased. For the cuprous oxide with the space group of $Pn\bar{3}m$, the numbers of oxygen ions per unit area on the (100) surface and on the (111) surface were estimated to be 2.78 and 8.83 nm^{-2}, respectively [9]. Because hydroxyl ions are a source of oxygen, pH determines the direction of the preferred orientation and the growth rate of each crystalline. Thus, as shown in XRD data of Figure 1(d), the Cu_2O layer prepared at pH 9 has a dominant peak at 42.35° corresponding to the (200) plane of cubic Cu_2O with cell parameter of 0.426 nm. On the other hand, the Cu_2O layers prepared at pHs 10 and 11 show a strong peak at 36.45° originating from the (111) Cu_2O. The change in the preferred orientation by bath pH also affects the grain shape, as shown in the SEM photographs. All the Cu_2O films were grown with columnar grains along the direction normal to the ITO/glass substrate and have a similar thickness of 3 μm. For pH 9 sample with the preferred orientation of (200), the crystal grains are very small and show a 4-sided structure, whereas the pH 10 and 11 samples with the (111) orientation show 3-faced pyramids rather than a 4-sided structure. Additionally, when the bath pH was increased to 12 by adding an amount of NaOH, the grain size of Cu_2O increased due to the lower nucleation density [20]. In this case, voids occurred and the complete coverage of the ITO substrate by the Cu_2O coating was quite delayed. As a result, high superfluous current directly flowed from the top electrode to the bottom ITO. The I-V curve shows the ohmic characteristic.

To confirm the conduction type of the Cu_2O layers deposited on the ITO substrates, the photoelectrochemical property of the layers was evaluated from a current-potential scan using linear sweep voltammetry (LSV). All samples of pH 9, 10, and 11 showed cathodic current, indicating the p-type characteristic. Figure 2 shows the I-V curves of the Cu_2O/ITO heterojunction for different pHs; these curves were used to determine for the optimal pH condition for the p-type Cu_2O layers. Although Hall Effect measurement is a useful and reliable method for confirming the electrical properties of thin films, it is difficult to use this measurement to evaluate the electrical resistivity of electrodeposited films requiring only conductive substrates such as ITO and metal substrates [21]. Alternatively, based on the I-V measurements using a two-point probe, the resistance values were obtained from a linear region of forward bias, 0.9~1.0 V. And then, the electrical resistivities of the Cu_2O layers were determined by

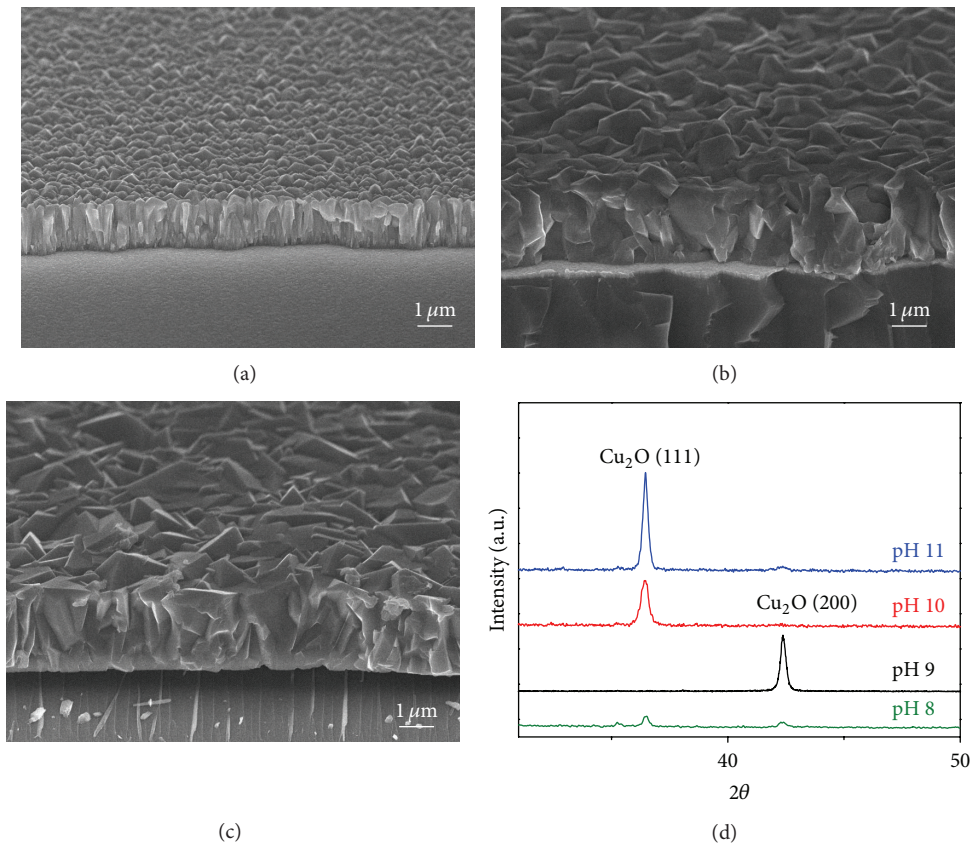

Figure 1: Tilt-view SEM images of the Cu_2O layers electrodeposited on ITO, which were synthesized at bath conditions of (a) pH 9, (b) pH 10, and (c) pH 11. (d) XRD patterns of the Cu_2O/ITO heterostructures.

using the area of the electrode and film thickness. Because the same pattern and electrodes were used, we could compare the electrical properties of the Cu_2O layers indirectly, as shown in the inset of Figure 2. The Cu_2O/ITO heterojunction formed at pH 9 showed very low current level; on the other hand, the Cu_2O/ITO heterojunctions formed at pHs 10 and 11 showed electrical rectification, despite the large leakage current at reverse bias. The electrical conductivity of the sample prepared with bath pH 11 was increased by approximately two orders, compared to that of the pH 9 sample. It is due to the increase in the carrier density of Cu_2O, based on the fact that copper vacancy and oxygen interstitials are controlled by the amount of hydroxyl concentration. The amount of hydroxyl concentration also affects the preferred orientation of the Cu_2O layer, and as a result, the Cu_2O layer with the (111) preferred orientation has lower resistivity than that with the (200) orientation.

To evaluate the absorbance of Cu_2O for photovoltaic applications, the optical absorption spectra of the Cu_2O layers prepared with bath pHs of 9, 10, and 11 in the Cu_2O/ITO heterojunctions were obtained, as shown in Figure 3. The Cu_2O layer deposited at pH 11 showed an absorption edge at 590 nm, and its band gap was estimated to be 2.1 eV by the following equation, because the Cu_2O has direct transition:

$$(\alpha h\upsilon)^2 = A\left(h\upsilon - E_g\right), \quad (2)$$

where α is the absorption coefficient and $h\upsilon$ is the incident photon energy. The results of $(\alpha h\upsilon)^2$ versus $h\upsilon$ are shown in the inset of Figure 3. The energy band gaps of the Cu_2O layers prepared at pHs 9 and 10 were estimated to be 2.25 and 2.1 eV, respectively. Although the electrodeposited layers were all identified as Cu_2O layers of cubic structure by XRD, the layers in the pH 9 and 10 samples showed difference in band gap energy of almost 0.15 eV. Different bath pHs resulted in different reduction potentials, as confirmed by the Pourbaix diagram, resulting in different overpotentials. Finally, bath pH determined the preferred orientation, crystallinity, and crystalline size of the Cu_2O layer. Based on the absorbance, the absorption efficiency of the Cu_2O layer prepared at pH 11 was higher than those of the other samples. Thus, we deposited Cu_2O layers at pH 11 as the absorber layers of solar cells.

Figure 4(d) shows the schematic diagram of the solar cell structure based on Cu_2O/ZnO nanowire heterojunction. The Cu_2O was electrodeposited as the absorber layer at pH 11 and 60°C under the applied potential of −0.4 V. For comparison, superstrate Cu_2O/ZnO thin film solar cell was also fabricated with 300 nm ZnO grown by ALD (Figure 4(a)). The Cu_2O/ZnO nanowire solar cell had 1200 nm nanowires grown by MOCVD (Figure 4(b)). The ZnO film was formed on the ITO as an electron injection layer of electrical resistivity of 3×10^{-1} Ω·cm. To fabricate the Cu_2O/ZnO

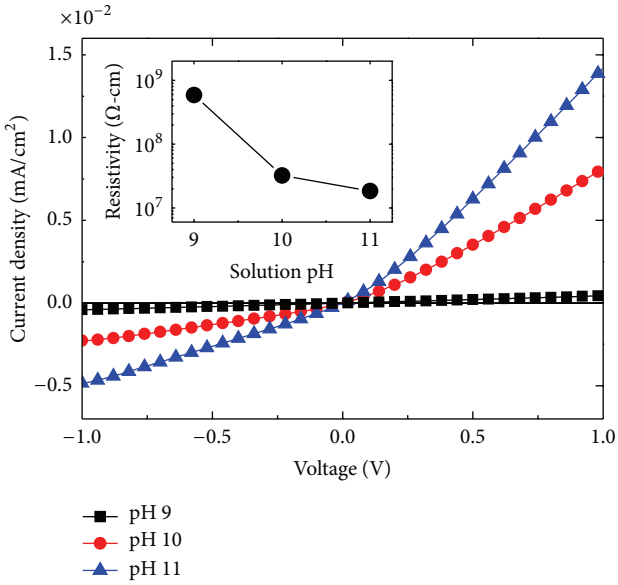

FIGURE 2: The current-voltage (I-V) characteristics of the Cu_2O/ITO heterojunctions with Cu_2O layers that were grown at different pHs. The inset shows the electrical resistivities of Cu_2O layers according to bath pH.

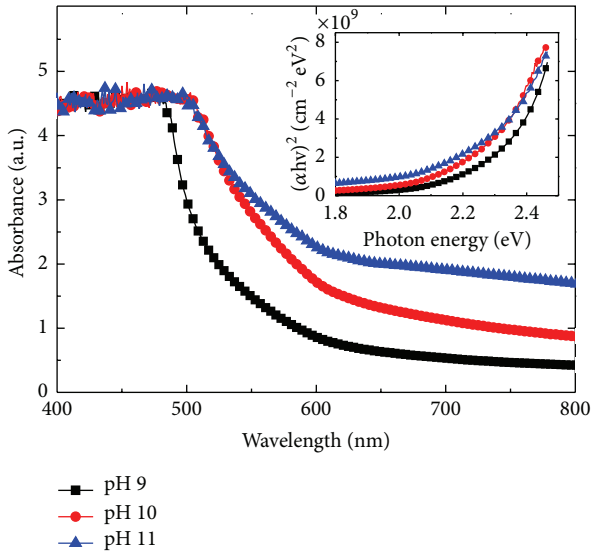

FIGURE 3: Absorbance spectra of the Cu_2O/ITO heterostructures deposited at different pHs. The inset shows $(\alpha h\nu)^2$-$h\nu$ curves, which were used to calculate the optical band gaps of Cu_2O layers.

nanowire structure, the AZO layer was deposited by ALD on the ITO substrate for the vertical alignment of ZnO nanowire arrays. Also, the nanowire arrays prevent the direct junction of Cu_2O and ITO, which shows a Schottky barrier in pH 11. Figure 4(c) shows the cross-section image of the vertically arrayed ZnO nanowires. According to a previous study on electrodeposited Cu_2O layers, the carrier density is relatively low, 10^{13}~10^{14}/cm^3 [22]. Thus, the Cu_2O absorber layer required a thickness of approximately 3 μm, which is related to depletion width, to form a full built-in potential, even though the Cu_2O has a short charge collection length [23]. The p-type Cu_2O layer completely fills the gaps between the ZnO nanowires, preventing current flow between the ZnO and the top electrode. The Cu_2O on the ZnO nanowires has 3-sided pyramid shape, because of the (111) preferred orientation at pH 11, as shown in the inset of Figure 4(b).

Figure 5 shows the J-V curves for the Cu_2O/ZnO heterostructures with different ZnO structures under the dark and the AM 1.5 illumination. The Cu_2O/ZnO film heterojunction showed rectifying behavior and a photovoltaic performance of 0.13%, with short-circuit current (J_{SC}) of 1.63 mA/cm$_2$, open-circuit voltage (V_{OC}) of 0.3 V, and fill factor (FF) of 26%. In contrast, J_{SC}, V_{OC}, and FF of the Cu_2O/ZnO nanowire heterojunction were 2.87 mA/cm^2, 0.34 V, and 27.5%, respectively, and the conversion efficiency of this structure was 0.27%. This conversion efficiency is higher than that of the Cu_2O/ZnO nanowire solar cell fabricated by Hsueh et al. [15] but lower than the conversion efficiency (0.36%) of the electrodeposited Cu_2O/ZnO nanowire fabricated by Musselman et al. [14] which showed the best performance among Cu_2O/ZnO nanostructured solar cells.

To understand the higher J_{SC} of the nanostructure, external quantum efficiency (EQE) was measured, as shown in Figure 6. Compared with the Cu_2O/ZnO planar structure, the Cu_2O/ZnO nanowire heterojunction showed improved EQE. Particularly, at the region above 475 nm, more photocurrent was generated. The absorption coefficient of Cu_2O changed sharply at ~475 nm. Thus, the optical depth was just 150 nm below 475 nm and μm scale above 475 nm. This indicates that the proper thickness of the Cu_2O absorber to absorb long wavelength illumination is almost 3 μm. However, the charge collection length of the Cu_2O related to the minority carrier diffusion length is <1 μm, which is much less than the optical depth of Cu_2O above 475 nm [14]. Thus, the electrons generated farther away from the charge collection length will be recombined before arriving at the ZnO region. This is the reason for the low EQE of the bilayer Cu_2O/ZnO structure at long wavelengths. On the other hand, in the nanostructured solar cell, the p-n junction region is extended because the electrodeposited Cu_2O permeates through the gaps between the ZnO nanowires. This allows the electrons generated by light of long wavelength to effectively arrive at the Cu_2O/ZnO interface. Consequently, the EQE of the nanostructured solar cell at 475~600 nm is much higher than that of a planar solar cell and thus the higher J_{SC}. Although the previous studies on nanowire-based Cu_2O solar cells showed V_{OC} of ~0.21 V [14], our nanostructured solar cell showed V_{OC} of 0.34 V, which is similar to the V_{OC} reported for planar solar cells. The V_{OC} is generally determined by the built-in potentials of the p-type and n-type materials. It has been reported that the carrier density of electrodeposited Cu_2O is significantly low (~10^{13} cm^{-3}). And thus, as mentioned earlier, in a Cu_2O absorber of thickness of <3 μm, a full built-in bias is not formed due to an inadequate depletion layer [23]. In nanostructured solar cells with ZnO nanowire arrays,

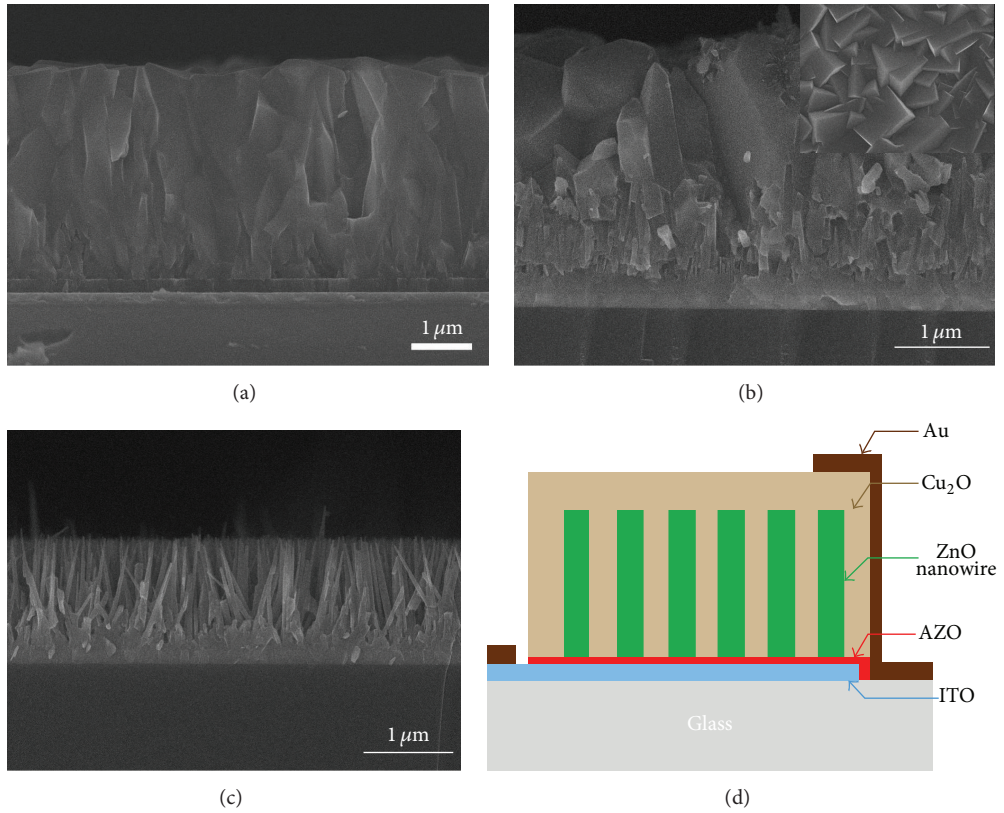

FIGURE 4: Cross-sectional SEM images of (a) Cu_2O/ZnO film, (b) Cu_2O/ZnO nanowire structures, and (c) ZnO nanowire arrays. (d) Schematic drawing of the Au/Cu_2O/ZnO nanowires/AZO/ITO/glass heterostructure solar cell. The inset shows plan-view SEM image of the Cu_2O layer deposited on the ZnO nanowires.

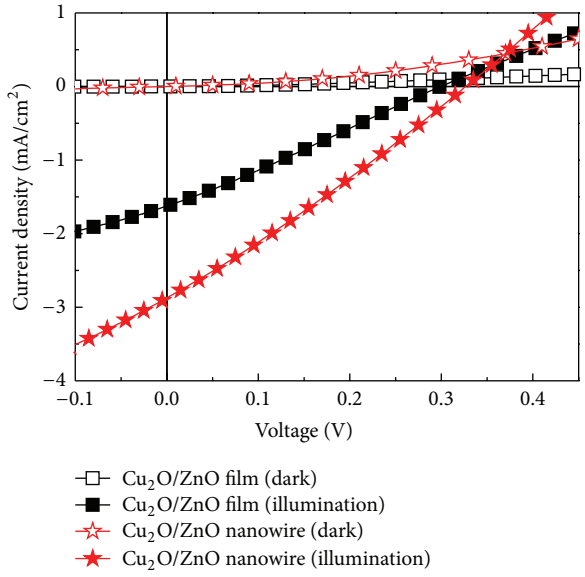

FIGURE 5: Dark and illumination I-V characteristics of Cu_2O/ZnO heterojunctions of planar and nanowire structure solar cells.

the reduced spacing between the nanowires suppresses the formation of the depletion layer in the Cu_2O. Therefore, it is expected that the V_{OC} in nanostructured solar cells is lower than that in planar solar cells. However, compared to the ZnO nanowires prepared by electrodeposition and hydrothermal deposition, the MOCVD grown ZnO nanowires in this study have high crystalline quality of a single crystal along the [0001] direction and high optical properties, which were confirmed in previous studies [24]. Because of the high crystallinity of the nanowires and the low lattice mismatch

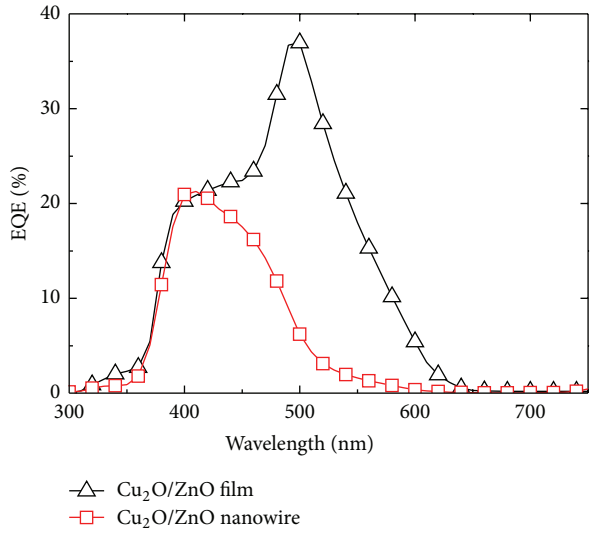

Figure 6: EQE curves of devices with different Cu_2O/ZnO heterojunction structures: planar and nanowire structure.

between ZnO (0001) and Cu_2O (111), it is expected that defect states at the Cu_2O/ZnO interfaces will be relatively low. These low defect states are responsible for the high V_{OC}, despite the introduction of nanowires in the Cu_2O/ZnO solar cells. Nevertheless, for the fabrication of high-efficiency Cu_2O/ZnO solar cells, low J_{SC} and FF should be improved, by suppressing the dark current and increasing the electrical conductivity of the electrodeposited Cu_2O film.

4. Conclusions

We investigated the effect of bath pH on the electrical, optical, and structural properties of electrodeposited Cu_2O layers for the development of inorganic oxide-based solar cells. The electrical resistivity and optical absorbance of the Cu_2O film deposited at constant pH 11 solution were suitable for the use of the Cu_2O film as the absorber layer of solar cells. We also fabricated a nanostructured Cu_2O/ZnO heterojunction solar cell at a previously confirmed optimal condition of the electrodeposition process. The Cu_2O layer prepared at pH 11 showed the (111) preferred orientation, increased electrical conductivity, and high optical absorption. We fabricated a Cu_2O/ZnO heterojunction solar cell consisting of ZnO nanowires with a high aspect ratio grown by MOCVD and Cu_2O layer electrodeposited to enhance the junction interface. The nanostructured solar cell showed higher conversion efficiency than the planar Cu_2O/ZnO solar cell. The enhanced long wavelength absorption due to the increased junction area was responsible for the increase in J_{SC}.

Acknowledgments

This research was supported by Basic Science Research Program through the National Research Foundation of Korea (NRF) funded by Ministry of Education, Science and Technology (2012-0001447) and by the National Research Foundation of Korea (NRF) Grant funded by the Korea government (MEST) (2012-003849). This work was also financially supported by the Energy International Collaboration Research & Development Program of the Korea Institute of Energy, Technology, Evaluation and Planning (KETEP) funded by the Ministry of Knowledge Economy (MKE) (2011-8520010050).

References

[1] L. C. Olsen, R. C. Bohara, and M. W. Urie, "Explanation for low-efficiency Cu_2O Schottky-barrier solar cells," *Applied Physics Letters*, vol. 34, no. 1, pp. 47–49, 1979.

[2] S. Wagner, J. L. Shey, P. Migliorant, and H. M. Kasper, "$CuInSe_2$/CdS heterojunction photovoltaic detectors," *Applied Physics Letters*, vol. 25, no. 8, pp. 434–435, 1974.

[3] R. S. Toth, R. Kilkson, and D. Trivich, "Preparation of large area single-crystal cuprous oxide," *Journal of Applied Physics*, vol. 31, no. 6, pp. 1117–1121, 1960.

[4] E. Fortin and D. Masson, "Photovoltaic effects in Cu_2O Cu solar cells grown by anodic oxidation," *Solid State Electronics*, vol. 25, no. 4, pp. 281–283, 1982.

[5] S. Yun Kim, C. Hyoun Ahn, J. Ho Lee et al., "p-channel oxide thin film transistors using solution-processed copper oxide," *ACS Applied Materials & Interfaces*, vol. 5, no. 7, pp. 2417–2421, 2013.

[6] R. N. Briskman, "A study of electrodeposited cuprous oxide photovoltaic cells," *Solar Energy Materials and Solar Cells*, vol. 27, no. 4, pp. 361–368, 1992.

[7] V. F. Drobny and L. Pulfrey, "Properties of reactively-sputtered copper oxide thin films," *Thin Solid Films*, vol. 61, no. 1, pp. 89–98, 1979.

[8] N. Fujimura, T. Nishihara, S. Goto, J. Xu, and T. Ito, "Control of preferred orientation for ZnO_x films: control of self-texture," *Journal of Crystal Growth*, vol. 130, no. 1-2, pp. 269–279, 1993.

[9] L. C. Wang, N. R. de Tacconi, C. R. Chenthamarakshan, K. Rajeshwar, and M. Tao, "Electrodeposited copper oxide films: effect of bath pH on grain orientation and orientation-dependent interfacial behavior," *Thin Solid Films*, vol. 515, no. 5, pp. 3090–3095, 2007.

[10] S. Hussain, C. Cao, G. Nabi, W. S. Khan, Z. Usman, and T. Mahmood, "Effect of electrodeposition and annealing of ZnO on optical and photovoltaic properties of the p-Cu_2O/n-ZnO solar cells," *Electrochimica Acta*, vol. 56, no. 24, pp. 8342–8346, 2011.

[11] M. Izaki, T. Shinagawa, K.-T. Mizuno, Y. Ida, M. Inaba, and A. Tasaka, "Electrochemically constructed p-Cu_2O/n-ZnO heterojunction diode for photovoltaic device," *Journal of Physics D*, vol. 40, no. 11, pp. 3326–3330, 2007.

[12] J. J. Loferski, "Theoretical considerations governing the choice of the optimum semiconductor for photovoltaic solar energy conversion," *Journal of Applied Physics*, vol. 27, no. 7, pp. 777–784, 1956.

[13] T. Minami, Y. Nishi, T. Miyata, and J. Nomoto, "High-efficiency oxide solar cells with ZnO/Cu_2O heterojunction fabricated on thermally oxidized Cu_2O sheets," *Applied Physics Express*, vol. 4, no. 6, Article ID 062301, 3 pages, 2011.

[14] K. P. Musselman, A. Wisnet, D. C. Iza et al., "Strong efficiency improvements in ultra-low-cost inorganic nanowire solar cells," *Advanced Materials*, vol. 22, no. 35, pp. E254–E258, 2010.

[15] T. J. Hsueh, C. L. Hsu, S. J. Chang, P. W. Guo, J. H. Hsieh, and I. C. Chen, "Cu_2O/n-ZnO nanowire solar cells on ZnO:Ga/glass templates," *Scripta Materialia*, vol. 57, no. 1, pp. 53–56, 2007.

[16] N. Yantara, N. Mathews, K. B. Jinesh, H. Kumar Mulmudi, and S. G. Mhaisalkar, "Modulating the optical and electrical properties of all metal oxide solar cells through nanostructuring and ultrathin interfacial layers," *Electrochimica Acta*, vol. 85, no. 15, pp. 486–491, 2012.

[17] D. C. Kim, B. O. Jung, Y. H. Kwon, and H. K. Cho, "Highly sensible ZnO nanowire ultraviolet photodetectors based on mechanical Schottky contact," *Journal of the Electrochemical Society*, vol. 159, no. 1, pp. K10–K14, 2012.

[18] A. Paracchino, J. Cornelius Brauer, J.-E. Moser, E. Thimsen, and M. Graetzel, "Synthesis and characterization of high-photoactivity electrodeposited Cu_2O solar absorber by photoelectrochemistry and ultrafast spectroscopy," *The Journal of Physical Chemistry C*, vol. 116, no. 13, pp. 7341–7350, 2012.

[19] M. Pourbaix, *Atlas of Electrochemical Equilibria in Aqueous Solutions*, NACE, 1974.

[20] C. M. McShane, W. P. Siripala, and K.-S. Choi, "Effect of junction morphology on the performance of polycrystalline Cu_2O homojunction solar cells," *Journal of Physical Chemistry Letters*, vol. 1, no. 18, pp. 2666–2670, 2010.

[21] K. Han and M. Tao, "Electrochemically deposited p-n homojunction cuprous oxide solar cells," *Solar Energy Materials and Solar Cells*, vol. 93, no. 1, pp. 153–157, 2009.

[22] K. Mizuno, M. Izaki, K. Murase et al., "Structural and electrical characterizations of electrodeposited p-type semiconductor Cu_2O films," *Journal of the Electrochemical Society*, vol. 152, no. 4, pp. C179–C182, 2005.

[23] K. P. Musselman, A. Marin, L. Schmidt-Mende, and J. L. MacManus-Driscoll, "Incompatible length scales in nanostructured Cu_2O solar cells," *Advanced Functional Materials*, vol. 22, no. 10, pp. 2202–2208, 2012.

[24] B. H. Kong, S. K. Mohanta, D. C. Kim, and H. K. Cho, "Optical and structural properties of ZnO thin films grown on various substrates by metalorganic chemical vapor deposition," *Physica B*, vol. 401-402, no. 15, pp. 399–403, 2007.